Iraqi Journal of Physics, 2024
https://doi.org/10.30723/ijp.v22i3.1272
Vol. 22, No. 4, PP. 11-20
P-ISSN: 2070-4003
E-ISSN: 2664-5548

Fabrication of Different Types of Photodetectors Based on Carbon Quantum Dots/Alq_3 Organic Material

Mina Mohammed Jawad[1a*] and Lamees A. Abdullah[1b]
[1]*Department of Physics, College of Science, University of Baghdad, Baghdad, Iraq*
[a*]Corresponding author: miiinamohammed@gmail.com

Abstract

In this work, the properties of the photodetector were improved by using carbon quantum dots (CQDs) and tris (8-hydroxyquinoline) aluminium (III) (Alq3) polymer when deposited on glass and silicon substrates. CQDs were prepared using an electrochemical method. Two methods of deposition were used; the first was drop casting, and the other was spin coating. The structural, electrical, and optical properties were studied. Measurements were made of the manufactured photoconductive detector's current-voltage (I–V) properties, photocurrent gain, response time, and quantum efficiency, responsivity. The constructed detector's performance was measured without light and using a 250-watt tungsten lamp, whose wavelength range was between 500 and 800 nm. The results showed that the best photodetector was when carbon quantum dots were used with Alq_3 deposited on a silicon substrate using the drop-casting method (CQD:Alq_3/Si). It was observed that the best gain, fastest rise, fall, and response times were 7.97, 0.98, 1.1, and 0.34 s, respectively.

Article Info.

Keywords:
Photodetector, Drop Casting, Spin Coating, Carbon Quantum Dots, Alq_3.

Article history:
Received: Mar. 30, 2024
Revised: Jul. 05, 2024
Accepted: Jul. 23, 2024
Published: Dec 01, 2024

1. Introduction

One exceptional category of optoelectronic devices is photodetectors (PDs). PDs produce electrical signals from photons or electromagnetic radiation. Depending on the active material, the absorbed photons produce electrons or electron-hole pairs [1-3]. Photodetectors operate in various light spectrums, including visible, infrared, ultraviolet (UV), and X-rays depending on the characteristics of the active material. Direct bandgap materials like silicon and II–VI semiconductors make up most of the primary components of PDs [4, 5]. Many studies have been conducted on the utilization of photodetectors in many applications, including environmental pollution monitoring, optical communication, flame detection, gas sensing, biomedical imaging, and semiconductor process control [6-10].

In the semiconductor field, the photodetection process relies on the generation of electron-hole pairs when exposed to light. In a semiconductor material, when the incident photons energy is equal to or greater than the bandgap, electrons are excited from the valence band to the conduction band and move freely through the crystal structure; electrical current can then flow when an electric field is applied. The presence of positively charged holes in the valence band also aids in electrical conduction under the influence of an electric field [11-13].

Organic semiconductor photodetectors have gained significant attention in recent years as viable alternatives to their inorganic counterparts. They offer advantages such as low temperature fabrication, simplicity, environmental friendliness, and cost-effectiveness. Organic materials can be chemically tailored to enhance absorption in the UV range and improve physical and chemical properties, thus facilitating efficient photon-to-electron conversion in UV photodetectors [14-18].

Carbon Quantum Dots (CQDs), zero-dimensional carbon nanostructures, have

garnered interest due to their unique optical, electrical, and optoelectronic characteristics. These chemically stable and biologically inert nanostructures exhibit excellent photostability and tunable optical properties akin to semiconductor quantum dots. Consequently, CQDs have found applications in photodetectors, light-emitting diodes (LEDs), solar cells, and photoelectrochemical cells [19-23].

This study employs tris(8-hydroxyquinoline) aluminum (Alq_3) and CQDs, as electron and hole transport materials, respectively. The organic blend of Alq_3:CQDs is utilized for photodetection purposes. The study focused on the fabrication of photodetectors based on CQDs:Alq_3 deposited on glass or silicon substrates using drop casting and spin coating deposition methods.

2. Materials and Methods

In this work, CQDs were prepared using the electrochemical method, which is the most effective method. 99.5 ml of ethanol (C_2H_5OH) was mixed with 0.5 ml of distilled water. To this solution, 0.3 g of sodium hydroxide (NaOH) was added and mixed well for two hours using a magnetic stirrer. This solution was poured into a 250 ml volumetric beaker and two graphite electrodes were placed inside the beaker, 2.5 cm apart. The electric current was set to 30 mA. To transfer ions from one electrode to another, the electrodes were rotated every 5 minutes. In this scenario, a milky white solution (mixture) was produced. After leaving it for five days, the color of the mixture changed to yellow-orange. Column chromatography was used to separate the CQDs from the resulting solution.

Drop casting technology was used to prepare CQDs films, 20 ml of diethyl ether ($C_2H_5OC_2H_5$) was mixed with 20 ml of silica gel (SiO_2); this solution was slowly mixed with 10 ml of petroleum ether (C_7H_{16}), then the final product was placed on the chromatographic column. The resulting filter was purified by adding quantum dots. which were then heated to a temperature of 50^o C. The films were of 600 nm thickness. The structural, electrical, and optical properties of the carbon quantum dots samples were studied in a previous work [24].

Eight different photodetector samples were manufactured as shown in Table 1. The samples were prepared using two different methods: drop casting and spin coating methods. In the drop casting method, a solution of CQDs:Alq_3 was deposited on a silicon substrate and then the rest of the solvent was evaporated at 60 °C for 30 minutes. In the spin coating, a solution was dropped onto a silicon substrate, which was spinned at a high speed. In this work, the speed was 1000 revolutions per minute which was applied for 30 seconds. The remaining solvent was evaporated at a temperature of 60 °C for 30 minutes. Fig. 1 represents the layers deposited on the different substrates

Table 1: Structure of photoconductor and preparation method.

Structure	**Sample preparation method**	**Structure**	**Sample preparation method**
CQD/Si	Drop casting	CQD:Alq_3/Si	Spin coating
CQD/glass	Drop casting	CQD:Alq_3/glass	Spin coating
CQD:Alq3/Si	Drop casting	Alq_3/Si	Drop casting
CQD:Alq3/glass	Drop casting	Alq_3/glass	Drop casting

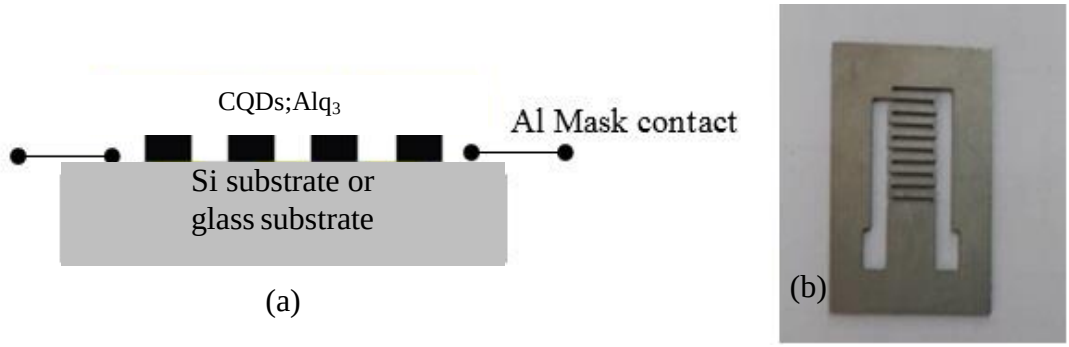

Figure 1: (a) The configuration of the photodoctor, (b) The Mask.

The samples preparation involved depositing CQDs after mixing them with Alq_3 on a glass or silicon substrate using one of the two methods, drop casting or spin coating. The three layers that make up the light detector were: the substrate either silicon or glass, the aluminum layer in the shape of a mask, as shown in Fig. 1b, and the third layer is the mixture of the two materials: CQD: Alq_3 depending on the deposition method.

A suitable setup was established to determine the detector parameters, I-V characteristics and response time of the photodetectors produced. The system consists of: a power supply, a digital multimedia connected to a personal computer (UNI-T UT803), a tungsten lamp with a wavelength 500-800 nm used to light the detectors and an optical power 250Watts, as shown in Fig. 2. Several parameters were measured for each sample using this setup, including gain, responsivity, quantitative efficiency and response time.

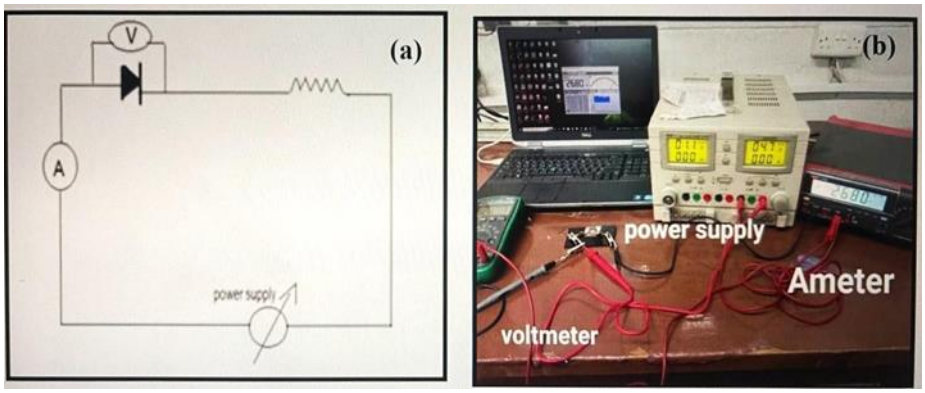

Figure 2: (a) Circuit diagram of (I-V) measurement of photoconductive device, (b) experimental setup of (I-V) measurement of photoconductive device.

3. Results and Discussion

3.1. I-V Characteristics of Photoconductor

The most frequently used method for characterizing devices is the I-V curve. This method measures the current in both dark and illumination conditions as a function of the photodetector device's voltage. Figs. 3-10 show the I-V characteristics. With bias voltage, the samples' I-V characteristics demonstrate an exponential rise in current due to decrease in the depletion layer width at the interface. The same measurement conditions (distance between the light source and the sample, wavelength and power of the light source, area of light on the sample, and distance between the electrodes mask) were applied to all samples in the photo response experiment. All measurements were done under illumination by a tungsten lamp with a wavelength in the range 500-800 nm and an optical power 250 W. Fig. 3a and b show the I-V characteristics for CQD/Si and CQD/glass, respectively (using drop casting deposition method) under dark and

tungsten lamp illumination. It can be noted that the current under illumination conditions is much higher than the current at the dark conditions. The maximum current values at 5 V under dark and illumination conditions are listed in Table 2. Fig. 4a and b show the I-V characteristics for CQD:Alq_3/Si and CQD:Alq_3/glass (drop casting method) under dark and tungsten lamp illumination. An increase in the current value up to 380 and 360 µA due to the presence of Alq_3 was noted.

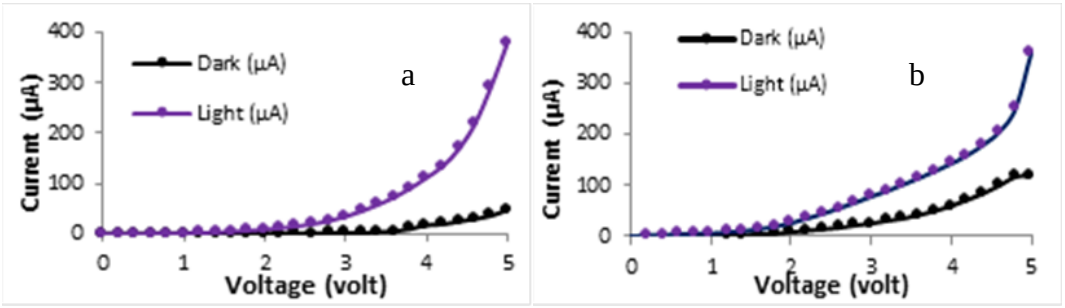

Figure 3: I-V characteristic of (a) CQD/Si, (b) CQD/glass using drop casting deposition.

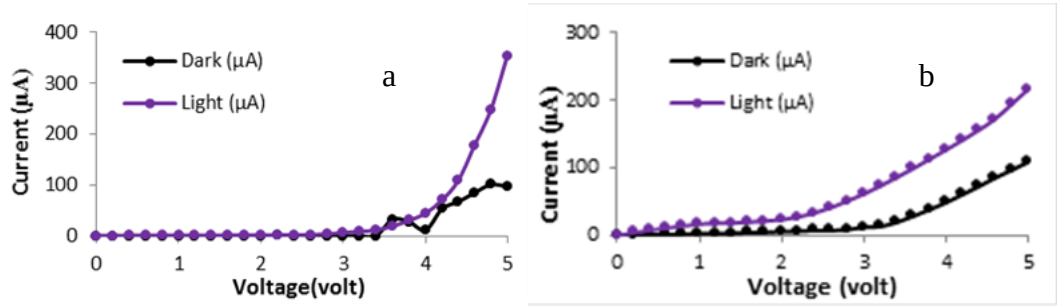

Figure 4: I-V characteristic of (a) CQD:Alq_3/Si, (b) CQD:Alq_3/glass using drop casting deposition.

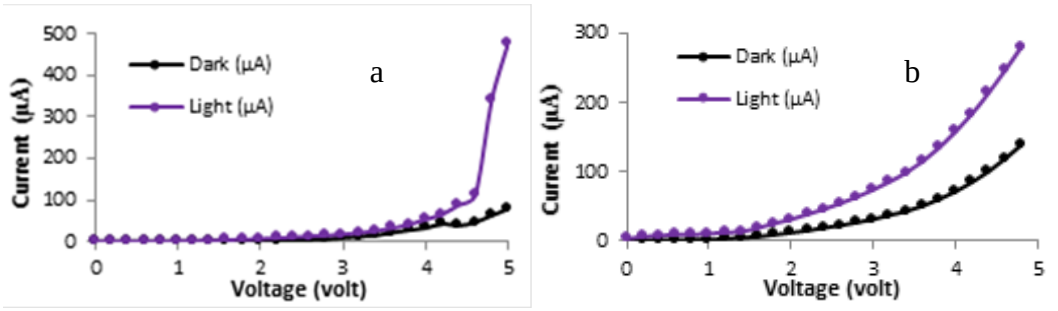

Figure 5: I-V characteristic of (a) CQD:Alq_3/Si, (b) CQD:Alq_3/glass using spin coating deposition.

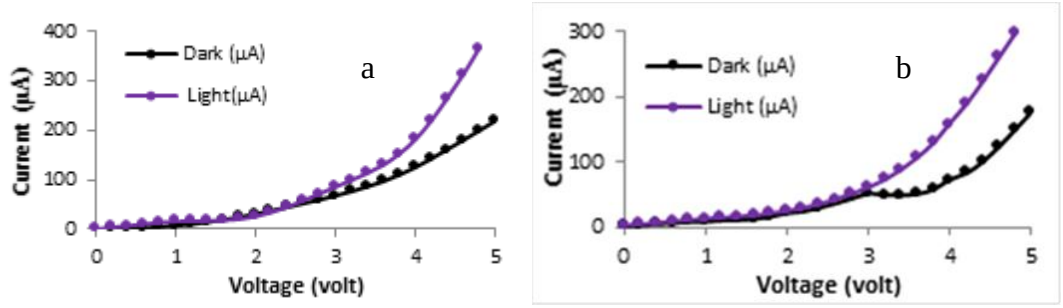

Figure 6: I-V characteristic of (a)Alq_3/Si, (b) Alq_3/glass using drop casting deposition.

Table 2: I-V characteristic of photodetectors manufacture.

Samples	**Maximum Current (μA) at illumination and 5 V**	**Maximum Current (μA) at Dark and 5 V**	**Sample**	**Maximum Current (μA) at illumination and 5 V**	**Maximum Current (μA) at Dark and 5 V**
CQD/Si	353.7	97.18	CQD:Alq_3/ Si (spin)	477.65	78.54
CQD/glass	216.08	108.66	CQD:Alq_3/ glass (spin)	280.34	138.82
CQD:Alq_3/Si (drop)	380.2	47.65	Alq_3/Si	366.17	199.36
CQD:Alq_3/glass (drop)	360.4	119.25	Alq_3/glass	297.81	150.17

The I-V characteristics of CQD:Alq_3/Si and CQD:Alq_3/glass (spin coating deposition) under dark and tungsten lamp illumination are shown in Fig. 5a and b, respectively. The figures show an increase in the photocurrent when the detector prepared by spin coating method, where the maximum current reach to 477.65 and 280.34 μA, respectively. The mix between two materials absorbs UV-Vis light. In case of using Si as a substrate to fabricate the CQD photoconductor, the current increase from 353.7 to 477.65 μA when adding Alq_3 to CQD. While Fig. 6a and b represents the I-V characteristic of the Alq_3/Si and Alq_3/glass (Drop Casting Deposition) under dark and tungsten lamp illumination. The maximum values of the photocurrent under tungsten lamp illumination were 366.17 and 297.81, respectively. In general, from Figs. 3 to 6, it can be observed that when the light source is switched off the dark photocurrent was low and the photocurrent increased greatly under tungsten lamp illumination.

3.2. Parameter of the Photoconductive Detector

From Figs. 11-18, the response time, rise time and fall time can be calculated.

3.2.1. Response Time (τ)

Response time represents the response speed to incident light, and it was calculated using equation (Rise time/2√2) [25]. The complex recombination mechanism of holes and electrons, and defects where carriers are bound and separated mostly affect this value. Transient response photodetectors are often very good at quickly detecting changes in light and situations demanding precise timing. The photodetector prepared using drop casting method (CQD:Alq_3/Si) showed the lowest response time (0.34 s), while the sample (CQD/Si) showed the highest response time (1.06 s), as shown in Table 3.

3.2.2. The Rise Time

After the light is switched on, the rise time is the time needed for the output signal to change from 10 % to 90 % of its maximum worth. The photodetector prepared using drop casting method on silicon substrate showed the lowest rise time (0.98 s), while sample of CQD/Si showed the highest rise time (3 s), as shown in Table 3.

3.2.3. The Fall Time

After the input light is suddenly turned off, the fall time is the time that takes for the output signal to descent from 90% to 10% of its peak worth. Fall time results are shown in Table (3).

3.2.4. The Responsivity (R)

The most important parameter of the photoconductive detectors is the responsivity. Responsivity of the prepared samples is determined using equation [26]

$$R = \frac{I_{ph}/A_1}{P_{out}} \quad (\mathbf{1})$$

where I_{ph} is the maximum value of current obtained from I-V curves at 5 V, A_1 is the area of the mask, which was 0.47 mm^2, and the P_{out} is the output power of the tungsten lamp, which was 150 W, as shown in Table 4. The sample of CQD/glass) showed the lowest responsivity of 0.88 A/W, while the sample prepared using spin coating method on silicon substrate showed the highest responsivity of 1.96 A/W.

3.2.5. Photocurrent Gain (G)

The photocurrent gain was computed by Eq. 2 for detector samples with visible absorption abilities to test their effects of enhancing photocurrent gain [27, 28]

$$G = \frac{\tau}{T_r} \quad (\mathbf{2})$$

where τ represents the carrier lifetime and T_r is the transit time, which is expressed by:

$$T_r = \frac{d^2}{\mu . V_B}$$

where d is the distance between the electrodes, μ is the majority carrier mobility, and V_B is the bias voltage applied to the sample. As shown in Table 4, the two samples deposited on Si substrate using drop casting and spin coating methods showed the highest photocurrent gain of 7.97 and 6.08, respectively.

3.2.6. Noise Equivalent Power (NEP)

Noise Equivalent Power, was calculated using the given equation [29, 30]

$$NEP = \frac{\sqrt{4\, k_B T\, \Delta f / R_S}}{R_d} \quad (\mathbf{3})$$

$$R_d = \frac{1}{I_d} \quad (\mathbf{4})$$

where K_B represents Boltzmann constant 1.38×10^{-23}J/K, T represent room temperature (300 K), Δf is the noise bandwidth and equal to 1Hz. The sample prepared using drop casting method on silicon substrate showed the lowest noise equivalent power of 2.93×10^{-9} W, as shown in Table 4.

3.2.7. Detectivity (D) and Specific Detectivity (D*)

The detector detectivity was calculated using Eq. 5. It depends on the noise current [29, 30]

$$D = \frac{1}{NEP} \quad (\mathbf{5})$$

The specific detectivity was calculated using the following equation [14, 29] [29,30]

$$D^* = \frac{\sqrt{\Delta f\, A_2}}{NEP} \qquad (6)$$

where: A_2 is the effective area of the surface of the detector. Detectivity and specific detectivity results are shown in Table 4.

3.2.8. Quantum Efficiency (η)

Quantum efficiency is related to the responsivity of the detector and is dependent on the wavelength of the illumination source. To obtain high quantum efficiency, it is important to have a surface recombination velocity as small as possible. It is calculated using the equation [30-32]

$$\eta = 1.24 \frac{R_S}{\lambda} \qquad (7)$$

where λ is the wavelength of the tungsten lamp, which was 532 nm because this wavelength had the maximum absorbance. Sample (CQD/SiO_2) showed the lowest quantum efficiency of 2.00×10^{-3}, while the sample prepared using spin coating method on silicon substrate showed the highest quantum efficiency of 4.57×10^{-3}.

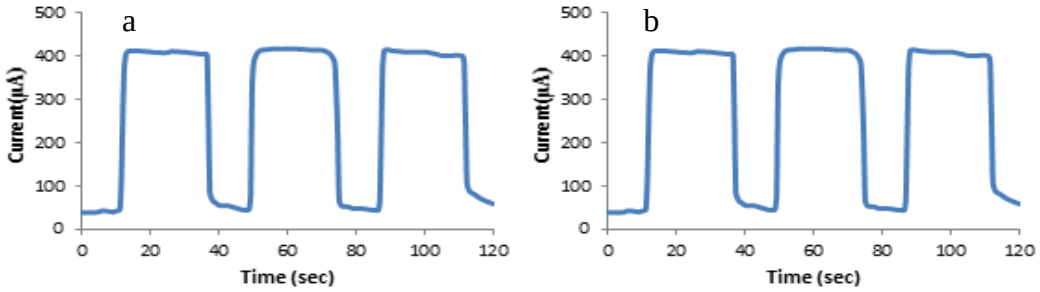

Figure 7: Photoresponse time of (a) CQD/Si detector, (b) CQD/glass detector using drop casting deposition.

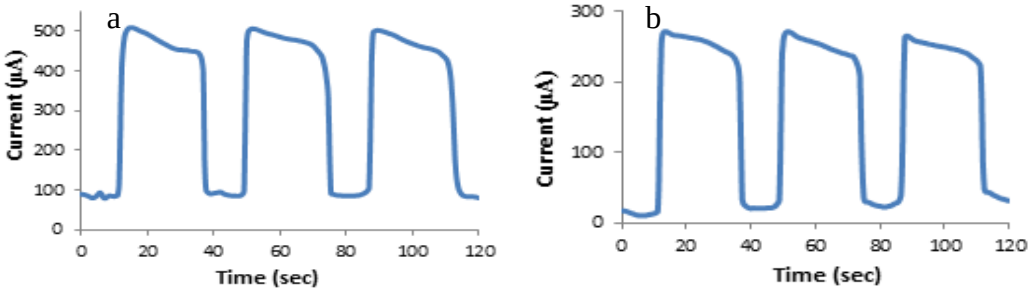

Figure 8: Photoresponse time of (a)CQD:Alq_3/glass detector, (b) CQD:Alq_3/Si detector using drop casting deposition.

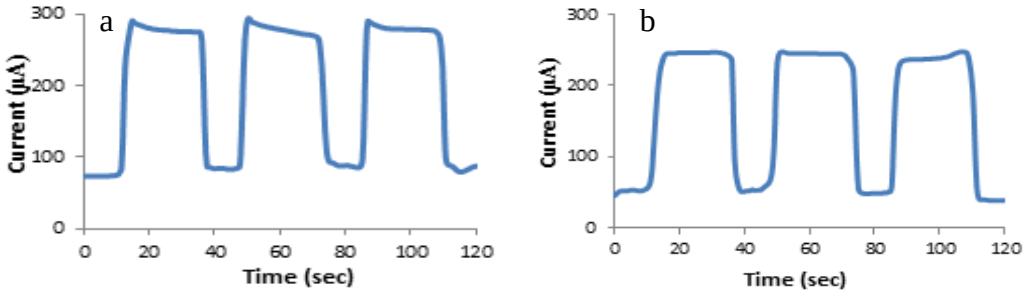

Figure 9: Photoresponse time of (a)CQD:Alq$_3$/glass detector, (b) CQD:Alq$_3$/Si detector using spin coating deposition.

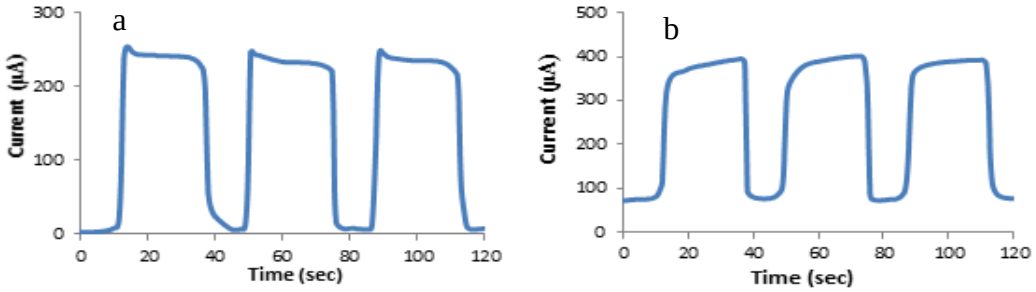

Figure 10: Phot response time of (a) Alq$_3$/Si detector, (b) Alq$_3$/glass detector using drop casting.

Table 3: Rise, fall and response time of the Photoconductors.

Samples	Rise Time (s)	Fall Time (s)	Response Time (s)
CQD/Si	3	1.3	1.06
CQD/glass	2.52	1.23	0.89
CQD:Alq$_3$/Si (drop)	0.98	1.1	0.34
CQD: Alq$_3$/glass (drop)	1.1	1.5	0.38
CQD: Alq$_3$/Si (spin)	1.8	2.55	0.90
CQD: Alq$_3$/glass (spin)	1.9	2.9	0.67
Alq$_3$/Si	1.48	2.62	0.52
Alq$_3$/glass	2.1	1.32	0.74

Table 4: Characteristics of the Photoconductors.

Samples	G	R_λ (A/W)	NEP (W)	I_n (A)	D (W^{-1})	D^* ($W^{-1}cm.Hz^{1/2}$)	η
CQD/Si	3.63	1.45	3.54×10^{-9}	3.64×10^{-11}	2.82×10^{8}	0.519×10^{8}	3.39×10^{-3}
CQD/glass	1.98	0.88	5.52×10^{-9}	5.08×10^{-11}	1.80×10^{8}	0.36×10^{8}	2.00×10^{-3}
CQD:Alq$_3$/Si (drop)	7.97	1.56	2.93×10^{-9}	6.14×10^{-11}	3.41×10^{8}	1.09×10^{8}	3.60×10^{-3}
CQD:Alq$_3$/glass (drop)	3.02	1.48	7.10×10^{-9}	5.96×10^{-11}	1.40×10^{8}	0.42×10^{8}	3.44×10^{-3}
CQD:Alq$_3$/Si (spin)	6.08	1.96	3.17×10^{-9}	4.04×10^{-11}	3.14×10^{8}	0.74×10^{8}	4.57×10^{-3}
CQD:Alq$_3$/glass (spin)	2.01	1.15	7.13×10^{-9}	5.14×10^{-11}	1.40×10^{8}	0.32×10^{8}	2.68×10^{-3}
Alq$_3$/Si	1.83	1.50	10.1×10^{-9}	5.09×10^{-11}	0.98×10^{8}	0.25×10^{8}	3.51×10^{-3}
Alq$_3$/glass	1.98	1.22	7.12×10^{-9}	4.74×10^{-11}	1.40×10^{8}	0.308×10^{8}	2.85×10^{-3}

Through the results of the characteristics of the photodetector of the prepared samples, it was found that the CQD:Alq_3/Si detector prepared using the drop casting method was the best because its rise, fall and response times were the shortest, as shown in Table 3. The CQD/Si photodetector showed the highest rise, fall and response time. The presence of Alq_3 had a positive effect on the operation of the photodetector. It is observed from Table 4 that photocurrent gain (G) was the highest (7.97) when the carbon quantum dots were added to Alq_3 deposited on a silicon substrate (CQD:Alq_3/Si) using the drop casting deposition. This result indicates an improvement in the work of the photodetector.

4. Conclusions

In this work, it was noticed from the I-V characteristics of the photodetectors samples that the current significantly increased due to the decrease in the width of the depletion layer at the interface. In general, it can be noticed that the photocurrent was low when the light source was turned off, and the photocurrent remarkably increased under illumination with a visible source. Through the results of the photodetector properties of the prepared samples, it was found that the response time and gain of the fabricated photoconductive detector (CQD:Alq_3/Si) prepared by the drop casting method were much higher than other detectors. The CQD/Si photodetector showed the highest rise and fall response times; the presence of Alq_3 improved the properties of the CQDs photodetectors.

Acknowledgements

The authors would like to thank the University of Baghdad - College of Science - Department of Physics for their assistance in carrying out this work.

Conflict of interest

Authors declare that they have no conflict of interest.

References

1. Z. Zhao, J. Liu, Y. Liu, and N. Zhu, J. Semicond. **38**, 121001 (2017). DOI: 10.1088/1674-4926/38/12/121001.
2. S. K. Batabyal, B. Pradhan, K. Mohanta, R. R. Bhattacharjee, and A. Banerjee, *Carbon Quantum Dots for Sustainable Energy and Optoelectronics* (Cambridge, US, Elsevier, 2023).
3. F. Huang, F. Jia, C. Cai, Z. Xu, C. Wu, Y. Ma, G. Fei, and M. Wang, Sci.Rep. **6**, 28943 (2016). DOI: 10.1038/srep28943.
4. H. Alzahrani, K. Sulaiman, A. Y. Mahmoud, and R. R. Bahabry, Synth. Metals **278**, 116830 (2021). DOI: 10.1016/j.synthmet.2021.116830.
5. S. Youssef, Y. M. El-Batawy, and A. A. Abouelsaood, J. Appl. Phys. **120**, 124506 (2016). DOI: 10.1063/1.4963287.
6. X. H. Nguyen, H. N. Luong, H. A. Pham, N. M. Nguyen, and V. Q. Dang, RSC Advan. **11**, 36340 (2021). DOI: 10.1039/D1RA06315D.
7. J. Liu, Y. Wang, H. Wen, Q. Bao, L. Shen, and L. Ding, Sol. RRL **4**, 2000139 (2020). DOI: 10.1002/solr.202000139.
8. A. Zhai, C. Zhao, D. Pan, S. Zhu, W. Wang, T. Ji, G. Li, R. Wen, Y. Zhang, Y. Hao, and Y. Cui, Nanomaterials **12**, 3084 (2022). DOI: 10.3390/nano12173084.
9. A. H. Mohammed, A. N. Naje, and R. K. Ibrahim, Iraqi J. Sci. **63**, 5218 (2022). DOI: 10.24996/ijs.2022.63.12.12.
10. S. I. Sharhan and I. M. Ibrahim, Iraqi J. Sci. **60**, 754 (2019). DOI: 10.24996/ijs.2019.60.4.9.
11. X. Sheng, C. Yu, V. Malyarchuk, Y.-H. Lee, S. Kim, T. Kim, L. Shen, C. Horng, J. Lutz, N. C. Giebink, J. Park, and J. A. Rogers, Advan. Opt. Mat. **2**, 314 (2014). DOI: 10.1002/adom.201300475.
12. D. Yang and D. Ma, Advan. Opt. Mat. **7**, 1800522 (2019). DOI: 10.1002/adom.201800522.

13. O. Adnan, A. N. Naje, and M. Midhat, Mat. Renew. Sust. Ener. **7**, 28 (2018). DOI: 10.1007/s40243-018-0135-7.
14. M. J. Shahlaa and O. Adnan, Instrum. Exp. Tech. **66**, 1106 (2023). DOI: 10.1134/S0020441223050342.
15. N. S. Hamzah and E. K. Hassan, Int. J. Nanosci. **22**, 2350028 (2023). DOI: 10.1142/s0219581x2350028x.
16. Z. Hassan and L. A. Abdullah, J. Opt. **53**, 428 (2024). DOI: 10.1007/s12596-023-01169-y.
17. P. Gu, Y. Yao, L. Feng, S. Niu, and H. Dong, Polym. Chem. **6**, 7933 (2015). DOI: 10.1039/C5PY01373A.
18. B. Kumar, B. K. Kaushik, and Y. S. Negi, Poly. Rev. **54**, 33 (2014). DOI: 10.1080/15583724.2013.848455.
19. Y. Wang and A. Hu, J. Mater. Chem. C **2**, 6921 (2014). DOI: 10.1039/C4TC00988F.
20. A. Hamid Abd and O. Adnan Ibrahim, Chem. Meth. **6**, 823 (2022). DOI: 10.22034/chemm.2022.351559.1575.
21. K. a. S. Fernando, S. Sahu, Y. Liu, W. K. Lewis, E. A. Guliants, A. Jafariyan, P. Wang, C. E. Bunker, and Y.-P. Sun, ACS Appl. Mat. Inter. **7**, 8363 (2015). DOI: 10.1021/acsami.5b00448.
22. N. A. Abd and O. A. Ibrahim, J. Opt. **53**, 2757 (2024). DOI: 10.1007/s12596-023-01462-w.
23. L. A. Essa and R. K. Jamal, J. Opt. **53**, 1574 (2024). DOI: 10.1007/s12596-023-01328-1.
24. M. M. Jawad and L. A. Abdullah, J. Opt., (2024). DOI: 10.1007/s12596-024-01687-3.
25. M. S. Mahdi, K. Ibrahim, N. M. Ahmed, A. Kadhim, S. A. Azzez, F. I. Mustafa, and M. Bououdina, Mat. Res. Expr. **4**, 105033 (2017). DOI: 10.1088/2053-1591/aa91e4.
26. M. W. Eesa, Iraqi J. Phys. **14**, 129 (2019). DOI: 10.30723/ijp.v14i31.180.
27. I. M. Ibrahim and A. H. Khalid, Baghdad Sci. J. **15**, 0441 (2018). DOI: 10.21123/bsj.2018.15.4.0441.
28. S. M. Sze, Y. Li, and K. K. Ng, *Physics of Semiconductor Devices* (Hoboken, New Jersey, John Wiley & Sons, 2021).
29. Z. H. Ali and L. A. Abdullah, Chem. Meth. **7**, 307 (2023). DOI: 10.22034/chemm.2023.379131.1636.
30. I. a. K. Hamad, Rana Ismael

Raoof, Asmaa Mohmmed Baghdad Sci. J. **16**, 1036 (2019). DOI: 10.21123/bsj.2019.16.4(Suppl.).1036.

31. H. Sadik, W. R. Saleh, N. M. H. Hadi, and N. Kadhum, Iraqi J. Sci. **58**, 868 (2022). DOI: 10.24996.ijs.2017.58.2B.11.
32. C. Li, W. Huang, L. Gao, H. Wang, L. Hu, T. Chen, and H. Zhang, Nanoscale **12**, 2201 (2020). DOI: 10.1039/C9NR07799E.

تصنيع انواع مختلفة من الكواشف المعتمدة على الكاربون الكمي النقطي لمادة عضوية Alq_3

مينا محمد جواد[1] ولميس عبد الكريم عبد الله[1]
[1]قسم الفيزياء، كلية العلوم، جامعة بغداد، بغداد، العراق

الخلاصة

في هذا العمل، تم تحسين خصائص الكاشف الضوئي باستخدام النقاط الكربونية الكمية (CQDs) وبوليمر الألومنيوم (III) ثلاثي (8-هيدروكسي كوينولين) (Alq3) عند ترسيبه على ركائز زجاجية وسيليكونية. تم تحضير CQDs باستخدام طريقة كهروكيميائية. استُخدمت طريقتان للترسيب؛ الأولى هي الصب بالقطرة والأخرى هي الطلاء بالدوران. تمت دراسة الخواص الهيكلية والكهربائية والبصرية. أُجريت قياسات لخصائص التيار-الجهد (I-V) للكاشف الموصّل الضوئي المصنّع، وكسب التيار الضوئي، وزمن الاستجابة، والكفاءة الكمية، والاستجابة. تم قياس أداء الكاشف المُصنَّع بدون ضوء وباستخدام مصباح تنجستن بقدرة 250 وات، وكان نطاق الطول الموجي بين 500 و800 نانومتر. أظهرت النتائج أن أفضل كاشف ضوئي كان عند استخدام النقاط الكربونية الكمية الكربونية مع Alq3 المودعة على ركيزة من السيليكون باستخدام طريقة الصب بالإسقاط (CQD:Alq3/Si). ولوحظ أن أفضل كسب وأسرع ارتفاع وانخفاض وأزمنة استجابة كانت 7.97 و0.98 و1.1 و0.34 ثانية على التوالي.

الكلمات المفتاحية: الكاشف الضوئي، الصب المسقط، الطلاء الدوراني، نقاط الكاربون الكمومية، Alq3.